Stability and Controlled Composition of Hexagonal WO_3

Imre Miklós Szilágyi,*,† János Madarász,‡ György Pokol,‡ Péter Király,§ Gábor Tárkányi,§ Sami Saukko,|| János Mizsei,⊥ Attila L. Tóth,# András Szabó,▽ and Katalin Varga-Josepovits○

Materials Structure and Modeling Research Group of the Hungarian Academy of Sciences and Department of Inorganic and Analytical Chemistry, Budapest University of Technology and Economics, H-1111 Budapest, Szt. Gellért tér 4, Hungary, Institute of Structural Chemistry, Chemical Research Center of the Hungarian Academy of Sciences, H-1025 Budapest, Pusztaszeri út 59-67, Hungary, Microelectronics and Materials Physics Laboratories, University of Oulu, FIN-90014 Oulu, Finland, Department of Electron Devices, Budapest University of Technology and Economics, Goldmann Gy. tér 3, Budapest H-1521, Hungary, Research Institute for Technical Physics and Materials Science, Hungarian Academy of Sciences, H-1121 Konkoly-Thege út 29-33, Budapest, Hungary, and Department of Organic Chemistry and Technology and Department of Atomic Physics, Budapest University of Technology and Economics, H-1111 Budapest, Budafoki út 8, Hungary

Received November 5, 2007. Revised Manuscript Received April 11, 2008

This paper discusses the formation of nanosized hexagonal tungsten oxide (h-WO_3) during the annealing of hexagonal ammonium tungsten bronze (HATB), $(NH_4)_{0.33-x}WO_{3-y}$. This process was investigated by TG/DTA-MS, XRD, SEM, Raman, XPS, and ^{1}H-MAS NMR analyses. Through adjusting the temperature and atmosphere of annealing HATB, the composition (W oxidation state, residual NH_4^+ and NH_3 content) of h-WO_3 could be controlled. The effect of composition on the conductivity and gas sensitivity of h-WO_3 was studied. New structural information was obtained about both HATB and h-WO_3. It was found that NH_4^+ and NH_3 could be situated at three different positions in HATB. Residual NH_4^+ and NH_3 in the hexagonal channels seemed to be vital for stabilizing h-WO_3: when they were completely released, the hexagonal framework collapsed. We propose that the structure of h-WO_3 cannot be maintained without some stabilizing ions or molecules in the hexagonal channels.

Introduction

Tungsten oxides have attracted much attention in the past few decades owing to their promising physical and chemical properties. As a wide bandgap *n*-type semiconductor, WO_3, is a potential candidate to be used in photoelectrochemical cells.[1,2] In contrast to TiO_2, which absorbs only UV light, WO_3 has absorption also in the visible spectrum, and this makes it a widespread material in photocatalysis.[3–6] WO_3 is also well-known as an effective catalyst in several acid-catalyzed reactions (isomerization and olefin polymerization, dehydration, and esterification of alcohols, etc.).[7–9] With its ability to change its color easily, WO_3 is the most researched material for chromogenic (electro-,[10–13] photo-,[14,15] gaso-,[16] and thermochromic[17,18]) devices. Its performance as a gas sensor to various gases (NH_3, NO_2, H_2S, etc.) is remarkable.[19–22] It also was reported that sodium doped WO_3 proved to be a high temperature superconductor with $T_c = 90$ K.[23]

Among tungsten oxides, hexagonal tungsten trioxide, h-WO_3, is of particular interest due to its open-tunnel structure and intercalation chemistry. It has been prepared

* Corresponding author. E-mail: imre.szilagyi@mail.bme.hu.
† Materials Structure and Modeling Research Group of the Hungarian Academy of Sciences, Budapest University of Technology and Economics.
‡ Department of Inorganic and Analytical Chemistry, Budapest University of Technology and Economics.
§ Chemical Research Center of the Hungarian Academy of Sciences.
|| University of Oulu.
⊥ Department of Electron Devices, Budapest University of Technology and Economics.
Hungarian Academy of Sciences.
▽ Department of Organic Chemistry and Technology, Budapest University of Technology and Economics.
○ Department of Atomic Physics, Budapest University of Technology and Economics.

(1) Grätzel, M. *Nature (London, U.K.)* **2001**, *414*, 338.
(2) Santato, C.; Odziemkowski, M.; Ulmann, M.; Augustynski, J. *J. Am. Chem. Soc.* **2001**, *123*, 10639.
(3) Kim, T.; Burrows, A.; Kiely, C. J.; Wachs, I. E. *J. Catal.* **2007**, *246*, 370.
(4) Arai, J.; Yanagida, M.; Konishi, Y.; Iwasaki, Y.; Sugihara, H.; Sayama, K. *J. Phys. Chem. C* **2007**, *111*, 7574.
(5) Georgieva, J.; Armyanov, S.; Valova, E.; Poulios, I.; Sotiropoulos, S. *Electrochem. Commun.* **2007**, *9*, 365.
(6) Baeck, S. H.; Choi, K. S.; Jaramillo, T. F.; Stucky, G. D.; McFarland, E. W. *Adv. Mater.* **2003**, *15*, 1269.
(7) Natile, M. M.; Tomaello, F.; Glisenti, A. *Chem. Mater.* **2006**, *18*, 3270.
(8) Onfroy, T.; Clet, G.; Houalla, M. *J. Phys. Chem. B* **2005**, *109*, 3345.
(9) Martín, C.; Solana, G.; Malet, P.; Rives, V. *Catal. Today* **2002**, *2844*, 1.
(10) Hepel, M.; Redmond, H.; Dela, I. *Electrochim. Acta* **2007**, *52*, 3541.
(11) Xue, B.; Peng, J.; Xin, Z.; Kong, Y.; Li, L.; Li, B. *J. Mater. Chem.* **2005**, *15*, 4793.
(12) Turyan, I.; Krasovec, U. O.; Orel, B.; Saraidorov, T.; Reinsfeld, R.; Mandler, D. *Adv. Mater.* **2000**, *12*, 330.
(13) Grandqvist, C. G. *Handbook of Inorganic Electrochromic Materials*; Elsevier: Amsterdam, 1995.
(14) Wang, S.; Feng, X.; Yao, J.; Jiang, L. *Angew. Chem., Int. Ed.* **2006**, *45*, 1264.
(15) He, Y.; Wu, Z.; Fu, L.; Li, C.; Miao, Y.; Cao, L.; Fan, H.; Zou, B. *Chem. Mater.* **2003**, *15*, 4039.
(16) Chen, H.; Xu, N.; Deng, S.; Lu, D.; Li, Z.; Zhou, J.; Chen, J. *Nanotechnology* **2007**, *18*, 205701.
(17) Lu, D. Y.; Chen, J.; Chen, H. J.; Gong, L.; Deng, S. Z.; Xu, N. S. *Appl. Phys. Lett.* **2007**, *90*, 41919.
(18) Durrani, S. M. A.; Khawaja, E. E.; Salim, M. A.; Al-Kuhaili, M. F.; Al-Shukri, A. M. *Sol. Energy Mater. Sol. Cells* **2002**, *71*, 313.

10.1021/cm800668x CCC: $40.75
Published on Web 05/21/2008

in several ways: by acidification and hydrothermal treatment (with various promoting reactants) of alkali tungstates,[24–28] by thermal evaporation and oxidation of tungsten metal,[29] by thermal[30,31] or wet chemical[32] oxidation of hexagonal ammonium tungsten bronze, by thermal oxidation of ammonium polytungstates,[33,34] and by spray pyrolysis using WCl_6 as the precursor.[35] Because of extensive research, now h-WO_3 is available in the form of nanoparticles,[24,25,30–33] nanofilms,[35] nanosheets,[26] nanowires,[27,28] and nanotubes.[29] Since most studies focused on the morphology of h-WO_3, little attention was paid to controlling its composition. However, the composition (amount of residual precursor molecules and ions, W/O ratio) of tungsten oxide nanosystems can be of great importance in some fields (e.g., gas sensors).

While it seems to be very difficult to control the amount of residual alkaline or ammonium ions in h-WO_3 by common wet chemical preparation methods, it is completely unsolved as to how to influence the oxidation state of W atoms in a reproducible way. Among the previously mentioned different preparation routes, we considered that it was the thermal oxidation of hexagonal ammonium tungsten bronze (HATB), $(NH_4)_{0.33-x}WO_{3-y}$, that might offer easy control of the composition of h-WO_3. We supposed that during heating this bronze, NH_3 and H_2O would release, and a hexagonal tungsten oxide structure would remain. It was thought that by adjusting the heating temperature and atmosphere of the precursor HATB, the composition (amount of residual NH_4^+ and NH_3, W/O ratio) of the product h-WO_3 might be influenced widely. However, this was only a hypothesis since this process has not been studied in detail yet (i.e., the release sequence of gaseous products and the changes in composition and crystalline structure during annealing were not investigated). Recently, we managed to prepare pure HATB, $(NH_4)_{0.07}(NH_3)_{0.04}(H_2O)_{0.09}WO_{2.95}$, by heating ammonium paratungstate tetrahydrate (APT), $(NH_4)_{10}[H_2W_{12}O_{42}]\cdot 4H_2O$, in H_2 for 6 h at 400 °C.[36] This good quality starting material, whose production was reproducible and reliable, and the supposed easy experimental control of its annealing encouraged us to prepare h-WO_3 from this HATB sample and to test as to whether the composition of h-WO_3 could be adjusted by this preparation route.

Table 1. Preparation Conditions of Selected Samples Prepared by Decomposing 1

sample	crystalline phase	atmosphere	temp (°C)
1	HATB		
2a	h-WO_3	air	400
2b	h-WO_3	air	470
2c	m-WO_3	air	600
3	h-WO_3	N_2	550
4	h-WO_3	10% H_2/Ar	550

In addition, it also was supposed that by studying this reaction, the role of residual ions in stabilizing the structure of h-WO_3 could be better understood. Recently, it was mentioned by Gu et al. that Li^+ ions helped to stabilize h-WO_3, but this statement was not supported by any experimental result or theoretical explanation.[27,28] Appropriate control of the annealing of HATB gave us the opportunity to vary the amount of residual NH_4^+ and NH_3 and to study if there was a correlation between their amount and the stability of h-WO_3.

Initially, we studied the thermal processes in oxidative (air) and inert (He) atmospheres with simultaneous TG/DTA and online evolved gas analysis (TG/DTA-MS) up to 900 °C to gain general insight into the formation of h-WO_3 from HATB. Intermediate solid products were analyzed by in situ and ex situ powder X-ray diffraction (XRD). Then, to obtain a detailed view of the composition and morphology of as-produced h-WO_3 samples, we used X-ray photoelectron spectroscopy (XPS), Raman spectroscopy, solid-state ^{1}H-MAS (magic angle spinning) NMR spectroscopy, and scanning electron microscopy (SEM). As a result, we obtained nanosized h-WO_3, and we found that its composition could be easily controlled. To show the influence of composition on applications of h-WO_3, the conductivity and gas sensitivity of as-prepared h-WO_3 samples with different compositions were measured.

Experimental Procedures

HATB, $(NH_4)_{0.07}(NH_3)_{0.04}(H_2O)_{0.09}WO_{2.95}$ (sample **1**), was prepared by heating APT, $(NH_4)_{10}[H_2W_{12}O_{42}]\cdot 4H_2O$, in H_2 for 6 h at 400 °C.[36] Table 1 provides the experimental conditions (decomposition atmosphere and temperature) for selected samples prepared from **1**.

Evolved gas analytical (TG/DTA-MS) measurements were conducted on an STD 2960 simultaneous DTA/TGA (TA Instruments) thermal analyzer coupled online to a Thermostar GSD 200 (Balzers Instruments) quadrupole mass spectrometer. The details of the TG/DTA-MS setup are discussed elsewhere.[37,38] Powder

(19) Espinosa, E. H.; Ionescu, R.; Llobet, E.; Felten, A.; Bittencourt, C.; Sotter, E.; Topalian, Z.; Heszler, P.; Granqvist, C. G.; Pireaux, J. J.; Correig, X. *J. Electrochem. Soc.* **2007**, *154*, 141.
(20) Ashraf, S.; Blackman, C. S.; Palgrave, R. G.; Parkin, I. P. *J. Mater. Chem.* **2007**, *17*, 1063.
(21) Stankova, M.; Vilanova, X.; Calderer, J.; Llobet, E.; Brezmes, J.; Gràcia, I.; Cané, C.; Correig, X. *Sens. Actuator, B* **2006**, *113*, 241.
(22) Polleux, J.; Gurlo, A.; Barsan, N.; Weimar, U.; Antonietti, M.; Niederberger, M. *Angew. Chem., Int. Ed.* **2006**, *45*, 261.
(23) Shengelaya, A.; Reich, S.; Tsabba, Y.; Müller, K. A. *Eur. Phys. J. B* **1998**, *12*, 13.
(24) Balázsi, C.; Wang, L.; Zayim, E. O.; Szilágyi, I. M.; Sedlackova, K.; Pfeifer, J.; Tóth, A. L.; Gouma, P. I. *J. Eur. Ceram. Soc.* **2008**, *28*, 913.
(25) Gerand, B.; Nowogrocki, G.; Guenot, J.; Figlarz, M. *J. Solid State Chem.* **1979**, *29*, 429.
(26) Oaki, Y.; Imai, H. *Adv. Mater.* **2006**, *18*, 1807.
(27) Gu, Z.; Ma, Y.; Yang, W.; Zhang, G.; Yao, J. *Chem. Commun. (Cambridge, U.K.)* **2005**, 3597.
(28) Gu, Z.; Li, H.; Zhai, T.; Yang, W.; Xia, Y.; Ma, Y.; Yao, J. *J. Solid State Chem.* **2007**, *180*, 98.
(29) Wu, Y.; Xi, Z.; Zhang, G.; Yu, J.; Guo, D. *J. Cryst. Growth* **2006**, *292*, 143.
(30) Schlasche, B.; Schöllhorn, R. *Rev. Chim. Miner.* **1982**, *19*, 534.
(31) Szilágyi, I. M.; Pfeifer, J.; Balázsi, C.; Tóth, A. L.; Varga-Josepovits, K.; Madarász, J.; Pokol, G. J. Therm. Anal. Calorim. 2007, accepted.
(32) Cheng, K. H.; Jacobson, A. J.; Wittingham, M. S. *Solid State Ionics* **1981**, *5*, 355.
(33) Han, W.; Hibino, M.; Kudo, T. *Solid State Ionics* **2000**, *128*, 25.
(34) Oi, J.; Kishimoto, A.; Kudo, T.; Hiratani, M. *J. Solid State Chem.* **1992**, *96*, 13.
(35) Ortega, J. M.; Martinez, A. I.; Acosta, D. R.; Magana, C. R. *Sol. Energy Mater. Sol. Cells* **2006**, *90*, 2471.
(36) Szilágyi, I. M.; Hange, F.; Madarász, J.; Pokol, G. *Eur. J. Inorg. Chem.* **2006**, *17*, 3413.
(37) Szilágyi, I. M.; Madarász, J.; Hange, F.; Pokol, G. *J. Therm. Anal. Calorim.* **2007**, *88*, 139.
(38) Madarász, J.; Szilágyi, I. M.; Hange, F.; Pokol, G. *J. Anal. Appl. Pyrol.* **2004**, *72*, 197.

XRD patterns of intermediate solid products of **1** decomposed in N_2 were measured by a PANalytical X'pert Pro MPD X-ray diffractometer equipped with an X'Celerator detector using Cu Kα radiation. In situ high temperature X-ray diffraction (HT-XRD) patterns of **1** in static air were collected by the same X-ray diffractometer in an Anton Paar HTK-2000 high temperature XRD chamber using Cu Kα radiation. The scanning time was ca. 3 min for each pattern, and the heating rate was 10 °C min^{-1} between XRD measurements. XPS spectra were collected by a VG Microtech instrument consisting of a XR3E2 X-ray source, a twin anode (Mg Kα and Al Kα), and a CLAM 2 hemispherical analyzer using Mg Kα radiation. Detailed scans were recorded with a 50 eV pass energy at (0.05 eV/1.5 s). The spectrometer was calibrated with the binding energy of the C1s line (284.5 eV). Raman spectra were collected by a Jobin Yvon Labram instrument attached to an Olympus BX41 microscope. A frequency doubled Nd:YAG laser (532 nm) was applied as an exiting source with 1 mW of applied power. The sample was located and examined with a 50× objective; thus, individual crystals could be examined (laser spot size was ca. 1.2 μm). The backscattered light collected by the objective was dispersed on an 1800 g/mm grating and detected by a 1024× 256 CCD detector. The measurement time was altered (3−100 s) according to the Raman activity of the samples.

Solid-state ^{1}H-MAS NMR experiments were carried out on a Varian NMR System spectrometer (600 MHz for ^{1}H) using a 3.2 mm HXY Varian/Chemagnetics probe. ^{1}H chemical shifts were referenced to adamantane (δ_iH = 0 ppm). Recycle delays were optimized by arrayed experiments, and proton pulse widths were calibrated for each sample. PW90 varied between 3 and 7 μs. Sixteen transients were acquired at a 12 kHz spinning rate, and a recycle delay of 20 s was used. Background suppression DEPTH[39] was employed to remove signals from the probe. SEM characterization was performed by a LEO-1550 FEG SEM instrument.

For resistance measurements of powder samples, a measurement cell with Cu electrical contact was prepared, into which a reproducible amount of powder (ca. 2 cm^3) could be loaded. Ten measurements were performed per sample with a Keithley 616 digital electrometer. To measure the gas sensitivity, sensors sheets with Pt electrical contact were produced by drop coating, for which Al_2O_3 sheets and dispersions of **2b** and **4** in ethanol were used. Sensing properties were tested to 10 ppm H_2S (in synthetic air) at 200 °C. More sensors could be placed into the testing instrument at the same time. This ensured that **2b** and **4** were tested at the same circumstances (i.e., they were reacted with the same gases, and the start and end of the tests were exactly at the same time for both sensors), which made the comparison of response and recovery times reliable.

Results and Discussion

Decomposition Sequence of Hexagonal Ammonium Tungsten Bronze. The simultaneous TG, DTG, DTA, and evolved gas analytical curves of **1** in helium are presented in Figure 1. On the basis of MS signals, the evolution of H_2O and NH_3 was detected (Figure 1). X-ray patterns of intermediates in He are shown in Figure 2.

In helium up to 200 °C, absorbed and chemisorbed H_2O evolved in two slightly endothermic, overlapping reactions (see the 1−2 DTG peaks in Figures 1 and 3). From 250 to 550 °C, H_2O and NH_3 were released in three endothermic, overlapping steps (see the 3−5 DTG peaks and the three

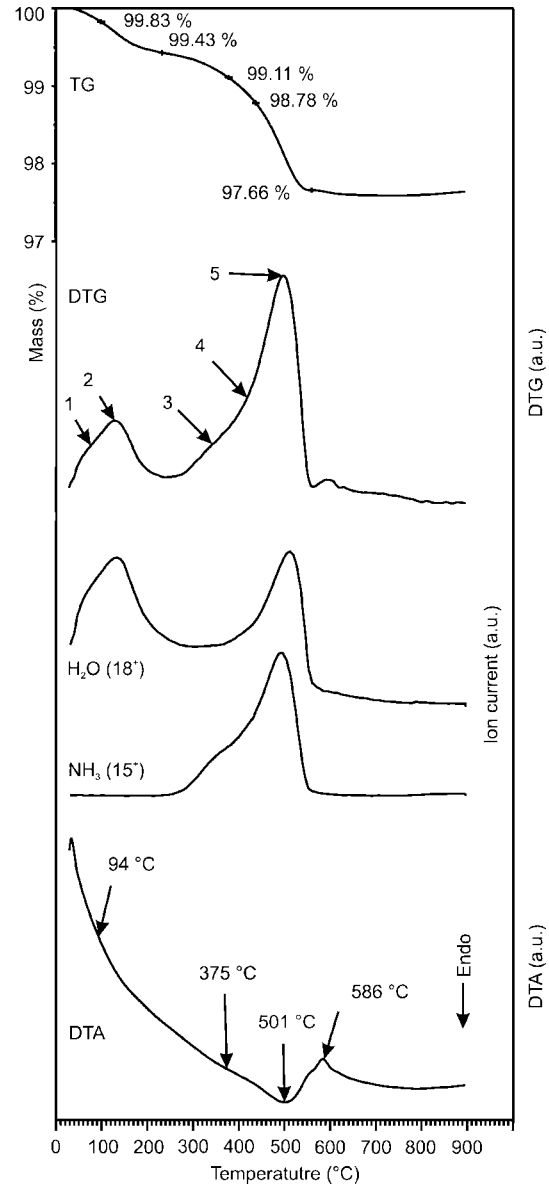

Figure 1. Simultaneous TG, DTG, DTA, and evolved gas analytical curves of **1** measured in He (130 mL min^{-1}, 10 °C min^{-1}, open Pt crucible, 106.5 mg).

overlapping peaks on the NH_3 release curve in Figures 1 and 3). Finally, between 550 and 600 °C, an exothermic heat effect was observed. At temperatures even higher, no further reaction took place.

We studied the structural changes, which accompanied these thermal processes, by XRD patterns. As more and more NH_3 left the sample, the structure of HATB (ICDD 42-0452) slowly shifted to h-WO_3 (ICDD 85-2460). This was followed by the increasing separation of the two peaks around 24°; by HATB, these peaks are at 23.702 and 24.041°, and by h-WO_3 they are at 23.286 and 24.305°. The hexagonal framework collapsed between 550 and 600 °C and transformed into monoclinic (m) WO_3 (ICDD 43-1035). The exothermic collapse and transformation (DTA peak at 586 °C)[2,31,32,40] of h-WO_3 into m-WO_3 can be rationalized by the greater stability of the latter.

(39) Cory, D. G.; Ritchey, W. M. *J. Magn. Reson.* **1988**, *80*, 128.

(40) Seguin, L.; Figlarz, M.; Pannetier, J. *Solid State Ionics* **1993**, *437*, 63.

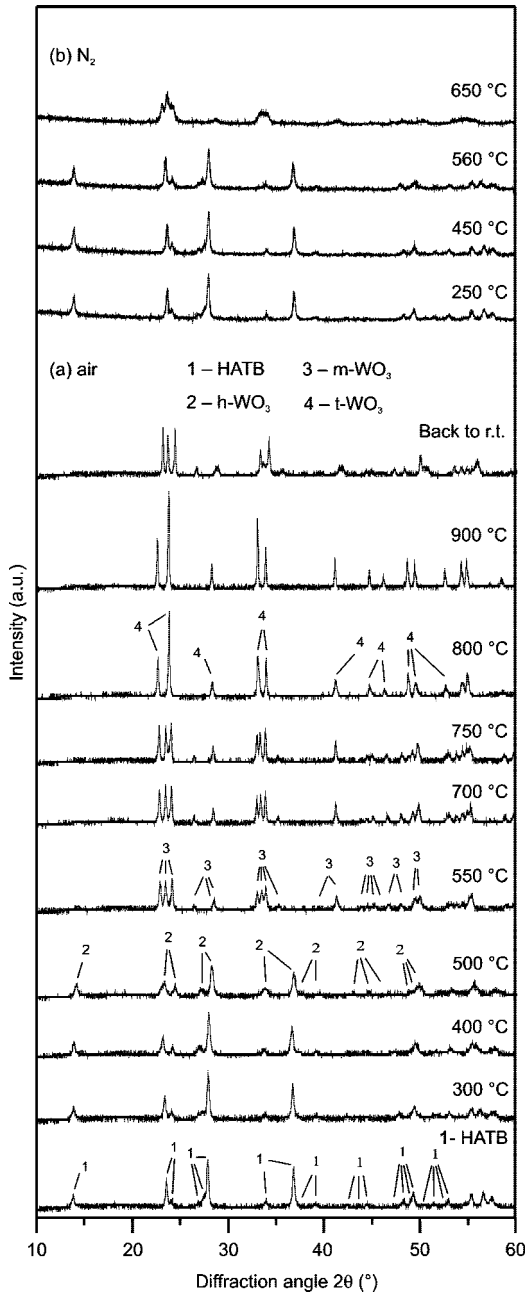

Figure 2. (a) In situ HT-XRD patterns of **1** decomposed in air and (b) ex situ XRD patterns of **1** decomposed in N_2.

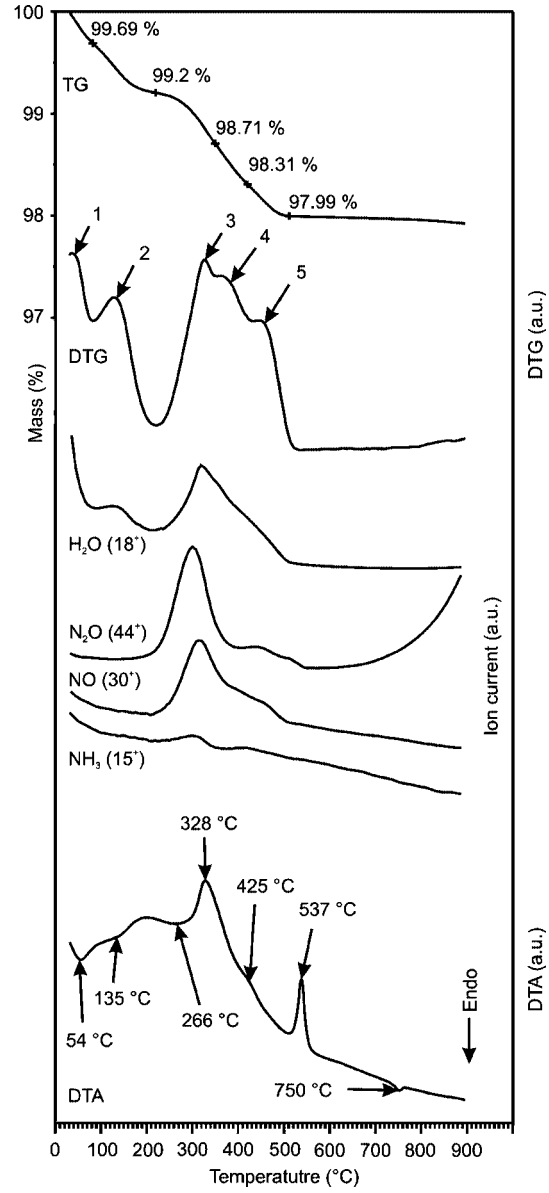

Figure 3. Simultaneous TG, DTG, DTA, and evolved gas analytical curves of **1** measured in air (130 mL min^{-1}, 10 °C min^{-1}, open Pt crucible, 104.3 mg).

In air, the processes were quite similar as in He (Figure 3). As a new feature, the evolution of nitrous oxides (NO, N_2O) was observed. This evolution was explained as combustion products of as-released NH_3. Since most of the NH_3 was burnt, the peaks on the NH_3 curve were quite weak, and the ratio of the corresponding DTG peaks was different as compared to that in helium. The combustion of NH_3 also was supported by the fact that previously it had been observed when ammonium paratungstate tetrahydrate, $(NH_4)_{10}[H_2W_{12}O_{42}]\cdot 4H_2O$, had decomposed in air.[38] Now, the DTA curve began as endothermic from 250 °C, due to the release of gases from the solid structure. But, the combustion of NH_3 was an exothermic reaction; thus, the DTA curve changed into an exothermic one after 300 °C (see the exothermic DTA peaks at 328 and 425 °C). There arose the question as to whether the combustion of NH_3 was catalyzed by either the Pt crucible[41] or the tungsten bronze structure.[42] To check the former case, we heated **1** in an Al_2O_3 crucible in air, but we did not observe any significant difference as compared to the processes in the Pt crucible.

As compared to He, another new feature in air was a reversible endothermic heat effect at 750 °C on the DTA curve. To explain it, we used in situ high temperature X-ray diffraction (HT-XRD), and by this we observed the reversible transformation from monoclinic into tetragonal (t) WO_3 (ICDD 85-0807) between 700 and 800 °C.[43] At 750 °C, the HT-XRD analysis showed a mixture of m- and t-WO_3, while by 800 °C, only t-WO_3 was present. The reversible m- and t-WO_3 transformation was reflected also by that, when the

(41) Pokol, G.; Leskelä, T.; Niinistö, L. *J. Therm. Anal.* **1994**, *42*, 343.
(42) *Gmelins Handbuch der Anorganischen Chemie: Stickstoff, System No. 4*; Verlag Chemie GmbH: Berlin, 1936; pp 645−683.
(43) Yamaguchi, O.; Tomihisa, D.; Kawabata, H.; Shimizu, K. *J. Am. Ceram. Soc.* **1987**, *70*, 94.

sample was cooling (not shown on Figure 3), there was an exothermic DTA peak around 700 °C, where t-WO_3 transformed back into m-WO_3. The fact that the m−t WO_3 reversible transformation did not appear in helium can be explained by the reduced WO_3 structure. While in air the W/O ratio was very close to the ideal 1:3 for m-WO_3, in helium, the m-WO_3 framework was distorted because of lacking oxygen atoms, and this could have blocked the formation of t-WO_3. The monoclinic framework can bear such small distortions, but the very well-ordered t-WO_3 cannot (in t-WO_3, tungsten atoms sit right at the center of each WO_6 octahedra on average[44]). This is why t-WO_3 could appear only in a fully oxidized (i.e., undistorted) environment.

Location of NH_4^+ Ions and NH_3 Molecules in HATB. We obtained new information about the location of ions in tungsten bronzes, as we studied the transformation of HATB to h-WO_3. In hexagonal tungsten bronzes, due to the special arrangement of corner-sharing WO_6 octahedra, triangular and hexagonal channels are formed along the structure. Alkaline (Na^+, K^+, Cs^+, etc.) or NH_4^+ ions are thought to be located in hexagonal channels.[44]

It was a new observation that NH_3 left the solid structure of HATB in three overlapping steps between 250 and 500 °C (see the three overlapping peaks on the NH_3 release curve in Figure 1 and NO and N_2O release curves in Figure 3, as well as the 3−5 DTG peaks in Figures 1 and 3). It is logical to deduce that NH_3 molecules were released in three different steps because they came from three different positions of HATB particles. We note that in HATB, both NH_4^+ ions and NH_3 molecules could be found.[36,45,46] When HATB was heated, on the one hand NH_3 was released simply. On the other hand, NH_4^+ left the solid structure in such a way that it combined with O and H atoms and formed NH_3 and H_2O molecules, which could then be released thermally. Therefore, as-released NH_3 originated from both NH_4^+ ions and NH_3 molecules bonded in HATB particles.

We considered two explanations for the origin of NH_3, which evolved in three different steps. On the one hand, it is possible that NH_3 was bonded more weakly in HATB than NH_4^+ since it could not form ionic bonds as NH_4^+. Therefore, at first, the NH_3 content of HATB could have been released, then in the next step, NH_4^+ ions bonded on the surface of particles and finally NH_4^+ ions situated in the hexagonal channels could have evolved. However, previous results showed that there was a long-range translational (diffusive) motion of protons between NH_4^+ and NH_3 in ammonium tungsten bronzes,[47] and it was suggested that there was a fast exchange equilibrium between NH_4^+ and NH_3 in HATB. This implies that it is very improbable that NH_3 could have evolved alone — leaving only NH_4^+ in the structure. It is more likely that NH_4^+ and NH_3 were released more or less parallel to each other. This was supported by ^{1}H-MAS NMR results (discussed in detail later), which showed that **2b** and **3** contained not only NH_4^+, as it would be expected by this explanation, but also NH_3.

On the other hand, the alternative explanation is that at first such NH_4^+ ions and NH_3 molecules could have left the solid structure, which were bonded the weakest and which were at the surface of the particles. In the last step, NH_4^+ and NH_3 could have come from those positions, where they were bonded the strongest (i.e., from the hexagonal channels of the crystallites). It is not completely understood as of yet from where NH_4^+ ions and NH_3 could have originated in the middle step. We suppose that they were situated either at a second kind of surface position, which was different from where NH_4^+ and NH_3 evolved in the first step, or at the disordered regions between the crystallite boundaries.

As discussed previously, the first hypothesis about the release of NH_3 in three different steps was not in accordance with theoretical considerations and ^{1}H-MAS NMR results. Therefore, we support the second explanation; however, we are aware that it is still a hypothesis. We note that although these results, which were provided by evolved gas analysis, need further support, they still are very useful since detection of these different ion and molecule positions in HATB has not been in the realm of other analytical methods yet. In this study, evolved gas analysis could turn out to be a successful analytical tool because NH_4^+ and NH_3 could be purged out of the structure thermally.

The knowledge of different ionic positions is also new information concerning tungsten bronzes in general. In practice, this observation can be used, for example, when the ion exchange property of tungsten bronzes is studied. In recent studies about the possible application of tungsten bronzes in nuclear waste treatment, it was reported that radioactive Cs^+ and Sr^{2+} were adsorbed successfully by hexagonal tungsten bronzes, but no exact mechanism was discussed.[48,49] Now, using thermal analysis and ammonium tungsten bronzes, it can be determined that cations at which positions have been exchanged (i.e., after an ion exchange reaction the population of NH_4^+ ions at the different – supposed – positions should change, which is to be shown by the intensity change of different peaks on the NH_3 release curve).

Formation of h-WO_3 with Controlled Composition. As **1** was heated, NH_3 and H_2O were released, and the structure as well as the composition slowly shifted toward h-WO_3. The change in composition meant that — according to the applied temperature and atmosphere — the oxidation state of tungsten atoms, the amount of residual NH_4^+ ions and NH_3 molecules, together with the bonds between atoms, all changed.

The oxidation state of tungsten atoms was investigated by XPS (Figure 4 and Table 2). Since **1** was partly reduced, W^{4+} and W^{5+} atoms also were observed besides W^{6+} atoms.[36] When **1** was heated in air at 470 °C, sample **2b** showed an almost fully oxidized structure, which also was supported by its yellow color. Compound **1** was oxidized in N_2 at 550 °C, but to a smaller degree, and sample **3** was

(44) Lassner, E.; Schubert, W. D. *Tungsten: Properties, Chemistry, Technology of the Element, Alloys, and Chemical Compounds*; Plenum Publishers: New York, 1999.
(45) Lunk, H. J.; Ziemer, B.; Salmen, M.; Heidemann, D. *Int. J. Refract. Met. Hard Mater.* **1993−1994**, *12*, 17.
(46) Lunk, H. J.; Salmen, M.; Heidemann, D. *Int. J. Refract. Met. Hard Mater.* **1998**, *16*, 23.
(47) Slade, R. C. T.; Dickens, P. G.; Claridge, D. A.; Murphy, D. J.; Halstead, T. K. *Solid State Ionics* **1990**, *38*, 201.
(48) Luca, C.; Griffith, C. S.; Drabarek, E.; Chronis, H. J. *Nucl. Mater.* **2006**, *358*, 139.

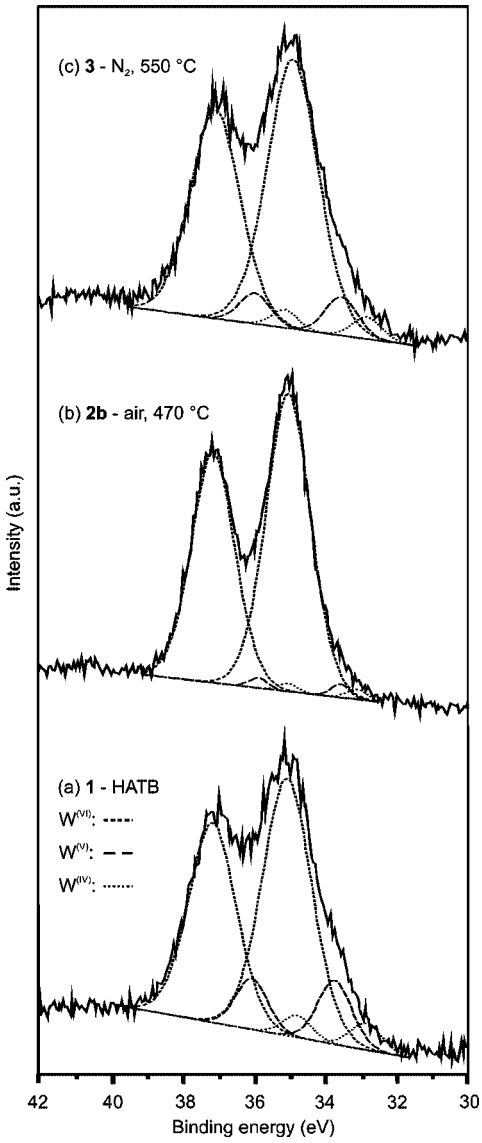

Figure 4. XPS spectra of (a) **1**, (b) **2b**, and (c) **3**.

Table 2. Ratio of W^{6+}, W^{5+}, and W^{4+} Atoms in HATB and in Its Decomposition Intermediates and Position of $W4f_{5/2}$ and $W4f_{7/2}$ Peaks

sample	W^{6+} (%)	W^{5+} (%)	W^{4+} (%)
1	80.9	13.8	5.4
2a	94.6	3.9	1.5
2b	96.8	1.8	1.4
3	88.1	7.9	4.0
4	77.3	15.9	6.8
$W4f_{5/2}$ peaks	35.0 eV	33.7 eV	32.8 eV
$W4f_{7/2}$ peaks	37.1 eV	36.0 eV	34.7 eV

greenish-yellow. Oxidation in inert atmosphere was caused perhaps by a small O_2 content of the inert gas or a leak in the furnace. Besides oxidative and inert atmospheres, we also studied the formation of h-WO_3 in a reductive (10% H_2/Ar) atmosphere at 550 °C. The results (which will be published in detail elsewhere) showed that in a reductive atmosphere, tungsten atoms were further reduced, and the color of sample **4** was blue.

We measured the amount of NH_4^+ ions and NH_3 molecules, which remained in the solid structure, by solid-state

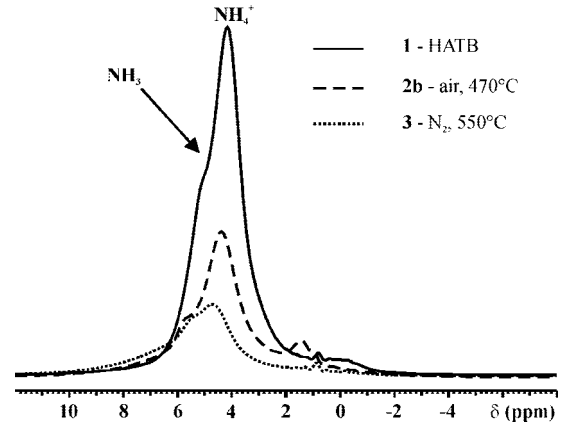

Figure 5. ^{1}H-MAS NMR spectra of intermediate solid products of **1** at 12 kHz MAS rate, 600 MHz.

^{1}H NMR spectroscopy[36,45,46] (Figure 5). ^{1}H-MAS NMR is the method of choice to extract direct information about the presence of these species, provided that signals from the probe background are eliminated.[39] We note that TG/DTA-MS measurements gave only indirect information about the presence of NH_4^+ and NH_3, while by XPS, Raman, or FTIR, we could not detect them at all. After curve fitting the ^{1}H-MAS NMR spectrum of **1**, the peaks at 4.5 and 5.6 ppm were assigned to NH_4^+ ions and NH_3 molecules, respectively. This assignment relies on the assumption that the peak positions do not interchange upon morphological changes. The ^{1}H-MAS NMR spectra showed that by raising the heating temperature of **1**, the amount of NH_4^+ ions and NH_3 molecules decreased, but they were still present in **2b** and **3**.

NMR spectroscopy also gave information about the bulk conductivity of h-WO_3 samples. HATB had both proton (because of H^+ containing species such as NH_3, NH_4^+, H_2O, and OH-group) and electron conductivity (because of electron hopping between W^{6+}, W^{5+}, and W^{4+} atoms).[50] On the one hand, upon releasing NH_3 it was expected that the proton conduction of all samples should reduce. On the other hand, it was supposed that as the number of reduced tungsten atoms increased in the reducing atmosphere, the electron conductivity of the sample should increase, while in air, it should decrease. Experimental data corroborated with these presuppositions. The samples exhibited rather different calibrations for the 90° proton pulse widths (pw90). Sample **4** required twice longer pulse widths than **2b**, which supports the higher bulk conductivity of reduced sample **4**.

Raman spectra also supported this latter observation (Figure 6). Compound **1** was highly crystalline, but since it conducted both electrons and protons,[50] its Raman bands were very broad. Therefore, it was difficult to assign the bands to certain vibrations, particularly the broad peak below 500 cm^{-1}, which might be deconvoluted into several deformation and lattice vibrations. The main band at 721 cm^{-1} and the shoulder at 654 cm^{-1} are assigned to stretching O−W−O modes, but other overlapping peaks also may be present. The small peak at 988 cm^{-1} should be attributed to

(49) Griffith, C. S.; Luca, V. *Chem. Mater.* **2004**, *16*, 4992.

(50) Huo, L.; Zhao, H.; Mauvy, F.; Fourcade, S.; Labrugere, C.; Pouchard, M.; Grenier, J. C. *Solid State Sci.* **2004**, *6*, 679.

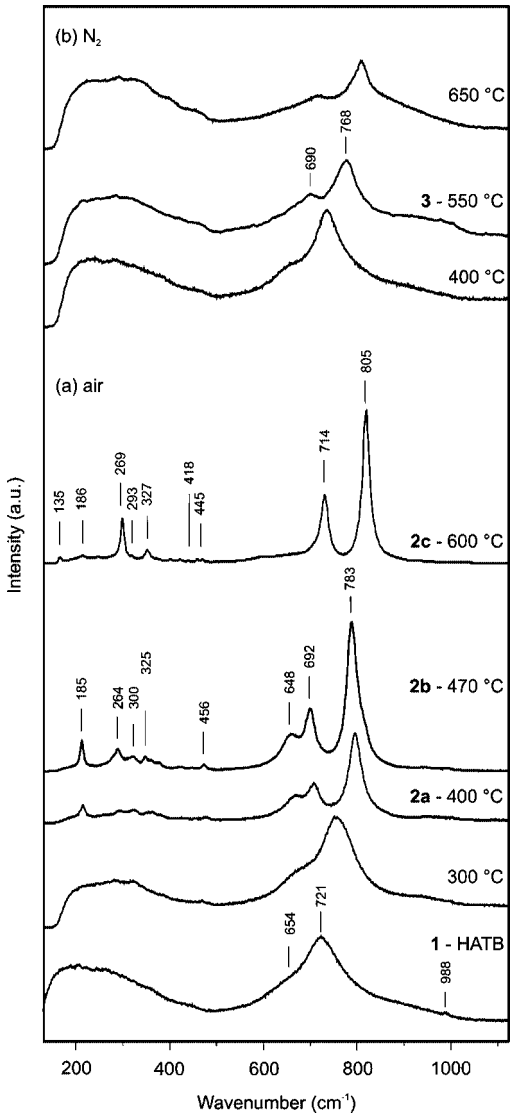

Figure 6. Raman spectra of intermediate solid products of **1** decomposed (a) in air and (b) in N_2.

a stretching mode of the terminal W═O.[51] Although this latter band is characteristic of tungsten oxide hydrates, it can appear in HATB because this compound adsorbs a relatively high amount of H_2O molecules[31] due to its active ionic surface.[45]

In N_2, Raman bands became moderately sharp due to moderate oxidization. In air, as the bulk conductivity of the sample decreased significantly due to more intense oxidization, Raman bands became much sharper. In air, the spectrum at 400 °C (sample **2a**) already showed a very oxidized sample, which matched well with XPS results (Table 2). By 470 °C, sample **2b** consisted of only h-WO_3, and the peaks were identified as typical Raman bands of h-WO_3 (Table 3). As the sample was heated further, traces of m-WO_3 already appeared at 500 °C, and at 600 °C, only the Raman bands of m-WO_3 (sample **2c**) were observable (Table 3). During annealing in N_2 and particularly in air, the oxidation of the sample also was shown by the shift of Raman bands. The chemical bonds with W^{6+} are stronger than those with W^{5+} and W^{4+}; therefore, Raman peaks for W^{6+}−O and W^{6+}═O appear at higher energies (i.e., higher wavenumbers).[51] In **1**, the main band was at 726 cm^{-1}, which shifted to greater wavenumbers as the samples became more oxidized: at 470 °C in air (sample **2b**), the maximum band was already at 786 cm^{-1}. In addition, the increase of this main peak (5 kcps with 100 s measurement time at 721 cm^{-1} for **1** and 20 kcps with 3 s measurement time at 783 cm^{-1} in **2b**) also showed a decrease in bulk conductivity.

Besides their composition, we also investigated the morphology of as-prepared h-WO_3 samples by SEM. The precursor of HATB (i.e., APT, $(NH_4)_{10}[H_2W_{12}O_{42}]\cdot 4H_2O$) was polycrystalline and consisted of micrometer scale particles. When **1** was produced from APT, the micromorphology was preserved, but the nanomorphology changed a great deal because 50−100 nm HATB particles were formed as HATB was crystallizing (Figure 7a) The annealing of **1** did not affect the morphology of the nanoparticles. The h-WO_3 samples produced both in air (sample **2b**) and in N_2 (sample **3**) also were built up by aggregated 50−100 nm particles (Figure 7b,c). This means that not only HATB but also h-WO_3 preserved the micromorphology of APT (shown in Figure 7c) and that the morphology of h-WO_3 can be controlled by the morphology of HATB or even APT.

In conclusion, our measurements showed that by controlling the heating temperature and atmosphere, and by selecting a HATB precursor with an appropriate particle size, the composition and morphology of h-WO_3 could be adjusted in a wide range. As a result, oxidized or reduced nanosized h-WO_3 samples can be prepared by this method, according to the application requirements.

To study as to whether the composition of h-WO_3 had an influence on its applications, the conductivity and gas sensitivity of as-prepared h-WO_3 samples with different compositions were measured. Indirectly Raman and ^{1}H-MAS NMR results showed such differences between the spectra of different h-WO_3 samples that could be interpreted as a result of differences in the bulk conductivity. We attempted to measure the conductivity/resistance of these samples directly. Measuring the resistance of powders has several difficulties (e.g., the amount and porosity of powders can influence the results a great deal). To reduce the effect of such mistakes, a measurement cell was prepared, into which reproducible amounts of powders could be loaded. Ten measurements were made per sample to reduce error, and it was found that the measurements were reproducible. The results showed that while the resistance of different h-WO_3 samples (14.3 ± 2.5, 15.5 ± 1.8, and 16.7 ± 4.2 MΩ for **2b**, **3**, and **4**, respectively) did not differ significantly, the resistance of HATB (sample **1**) was 2 orders of magnitude greater (1.25 ± 0.4 GΩ) than that of h-WO_3 samples. On the basis of this, we believe that the measured resistance of these powder samples is determined mainly by the surface connections of the particles rather than by the bulk properties. The significantly higher resistance of **1** should be in connection to that its surface contained much more NH_4^+, NH_3, and adsorbed H_2O. Therefore, while indirectly it was observed by Raman and ^{1}H-MAS NMR that the composition had an influence on the bulk resistance of different h-WO_3

(51) Ramana, C. V.; Utsunomiya, S.; Ewing, R. C.; Julien, C. M.; Becker, U. *J. Phys. Chem. B* **2006**, *110*, 10430.

Table 3. Raman Peaks of HATB and Its Decomposition Intermediates

Raman modes[2,51,54]	**1** (cm^{-1})	**2b** (cm^{-1})	**2c** (cm^{-1})	**3** (cm^{-1})
O−W−O stretching	654, 721	648, 692, 783	714, 805	690, 768
O−W−O deformation	between 200 and 500	264, 300, 325	269, 293, 327	between 200 and 500
lattice modes	below 200	184	135, 186	below 200
stretching of terminal W═O	988			
related to reduced W atoms		456		
others characteristic to m-WO_3			418, 445	

samples, direct resistance measurements did not show this, probably because the resistance of powder samples was determined more by the surface of the particles than by the bulk.

To investigate the correlation between the gas sensitivity and the composition of h-WO_3, gas sensors were prepared from oxidized (**2b**) and reduced (**4**) h-WO_3 and tested with H_2S. The results (Figure 8) showed that when 80% of the end signal was reached, the response and recovery times of **2b** (140 and 50 s, respectively) were 2.3−2.4 times shorter than with **4** (320 and 120 s, respectively). This was a significant difference, and it showed that the oxidized form of h-WO_3 is better for sensing H_2S and also that, in general, the composition had an impact on the gas sensitivity of h-WO_3.

Stability of Hexagonal WO_3. Usually, h-WO_3 is described as a metastable phase, and we propose what may stabilize it. According to our thermoanalytical and solid-state studies, h-WO_3 collapsed parallel to the final release of NH_4^+ ions and NH_3 molecules (i.e., parallel to that all NH_4^+ ions and NH_3 molecules left the hexagonal channels of the crystallites). This observation suggests that NH_4^+ and NH_3 in the hexagonal channels were vital for stabilizing the hexagonal structure; without them, the hexagonal tungsten oxide framework collapsed immediately.

On the basis of this, we suppose that in general some ions or molecules are needed in the hexagonal channels to maintain a hexagonal tungsten oxide structure (Figure 9). This hypothesis is supported by a recent study where the thermal stability of such h-WO_3 samples was investigated,[31] which were prepared from Na_2WO_4 and contained various amounts of residual Na^+. It was found that the h-WO_3 sample with a higher Na^+ content remained stable up to much higher temperatures than the one with a low Na^+ content. This result also shows that there is a correlation between the amount of residual ions and the stability of h-WO_3.

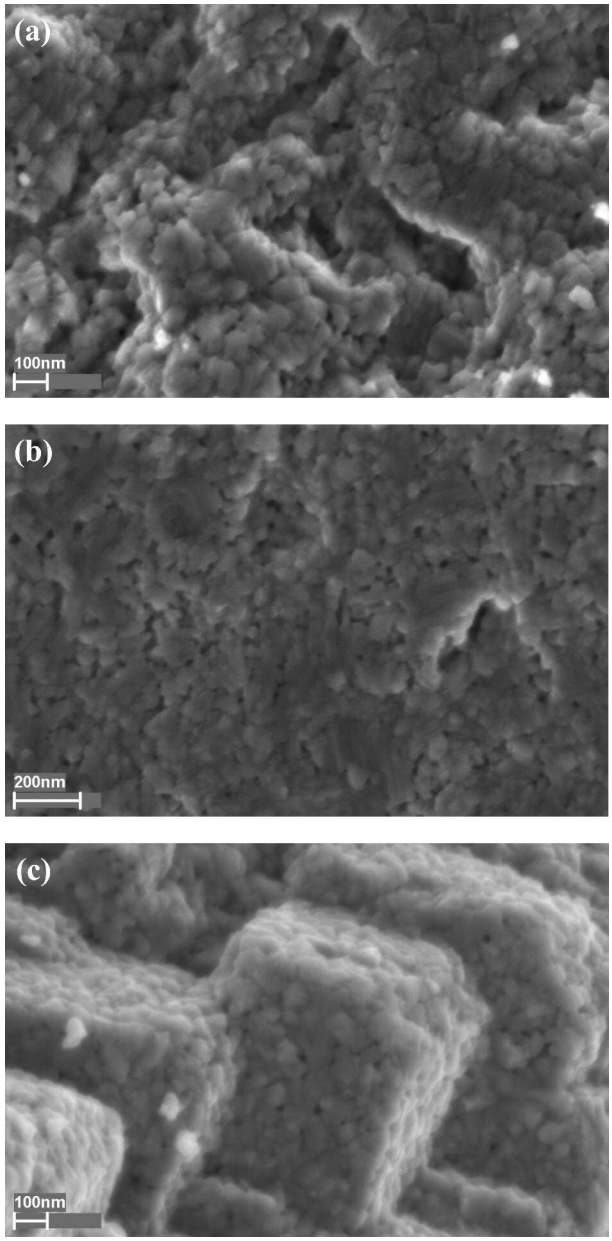

Figure 7. SEM images of (a) **1**, (b) **2b**, and (c) **3**.

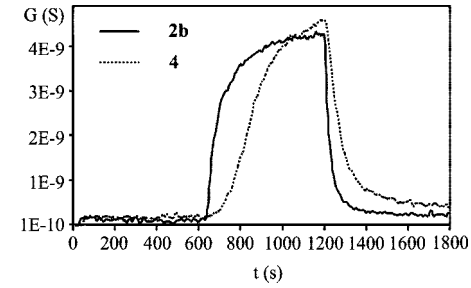

Figure 8. Sensitivity of **2b** and **4** to 10 ppm H_2S at 200 °C.

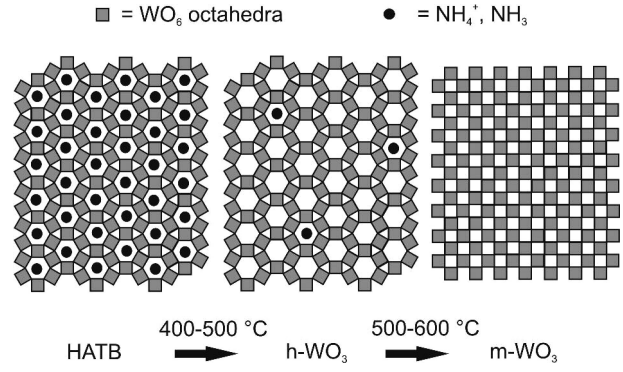

Figure 9. Phase transformations between HATB, h-WO_3, and m-WO_3.

Impurities are not only necessary to stabilize h-WO_3, but without a minimum amount of them, h-WO_3 cannot even form, as was shown recently.[25,52] In a common soft chemical preparation route of h-WO_3, HCl was added to Na_2WO_4, and H_2WO_4 formed, which after several washing steps transformed into $WO_3 \cdot 0.33H_2O$. After hydrothermal treatment, this phase transformed into h-WO_3, but only in the case if the Na^+ content of the precursor $WO_3 \cdot 0.33H_2O$ was larger than 160 ppm. This minimum amount of Na^+ was necessary for the formation of h-WO_3.

We can only hazard a guess as to the amount of necessary impurities in h-WO_3. As was mentioned, in Na^+ containing h-WO_3 samples, the minimum value was 160 ppm Na^+. However, in these samples, a significant amount of H_2O molecules also was present in the hexagonal channels.[31] In h-WO_3 samples containing NH_4^+ and NH_3, we attempted to determine the amount of stabilizing impurities by preparing several h-WO_3 samples at different temperatures in air, and we studied which contained only h-WO_3 and which contained its decomposition product, m-WO_3. The temperature limit for preparing monophase h-WO_3 from **1** was 470 °C. The sample at 470 °C (**2b**) contained ca. 0.11 wt % NH_4^+ and 0.04 wt % NH_3.[31] These amounts of minimum residual elements represent the overall amount of impurities; however, only a part of them is located in the hexagonal channels of crystallites.

How can such a small amount of ions or molecules stabilize the hexagonal tungsten oxide framework? Since in hexagonal tungsten bronzes ($M_{0.33-x}WO_{3-y}$) the hexagonal channels are filled if $x = 0$, it can be calculated that in the case of **2b**, <8% of the cavities in the hexagonal channels were filled by NH_4^+ ions or NH_3 molecules (Figure 9).

The stable form of WO_3 at room temperature (rt) is the orthorhombic/monoclinic phase, where the WO_6 octahedra are connected in a chessboard arrangement (Figure 9). In contrast to the monoclinic phase, the hexagonal form of WO_3 is metastable. We propose that the impurities stabilize the structure of h-WO_3 in such a way that they block the thermodynamically favored h−m transformation. Although the amount of impurities in h-WO_3 is usually quite low, they can have an observable effect on the crystalline structure. It was shown recently[53] that variations in the amount of residual Na^+ in h-WO_3 caused observable changes in lattice parameters (i.e., observable distortions in the lattice) and that they also influenced the kinetics of the formation of h-WO_3 from $WO_3 \cdot 0.33H_2O$ as well as the reduction of h-WO_3. We believe that in a similar way, even a low concentration of impurities can be enough for increasing the activation energy of the h−m transformation so much that it cannot take place at rt. So that the h−m transformation could occur, the network of corner sharing WO_6 octahedra has to be deformed at first, and some of the bonds have to be eliminated, which requires activation energy. Foreign ions or molecules may make the network of corner sharing WO_6 octahedra less flexible around themselves; therefore, it will be more difficult to deform these regions, and this requires a higher activation energy. At elevated temperatures, the atoms have a larger vibrational energy, and this can enable the structure to overcome the blocking effect of residual ions and molecules, and the h−m transformation can occur (Figure 9). This hypothesis predicts that the larger the amount of impurities is, the more intense their stabilizing effect is and thus the higher the temperature is, where the hexagonal framework collapses, and this corroborates with previous observations.[31]

Distortions in the crystalline structure due to oxygen deficiency may have a similar effect. We propose that they also can increase the stability of h-WO_3 and prolong the existence of the hexagonal structure. This might have occurred when **1** was heated in an inert atmosphere, where the hexagonal framework collapsed at a 50 °C higher temperature than in air.

Awareness concerning the presence of stabilizing ions and molecules in h-WO_3 is important because, in general, h-WO_3 is considered as a material that contains tungsten and oxygen only, and residual elements are mentioned only rarely.[27,28,31,52,53] But, based on our results, we believe that there is no such material that has an undistorted hexagonal structure and contains only tungsten and oxygen in stoichiometric amounts. In fact, to maintain the hexagonal tungsten oxide structure, some impurities are needed in the hexagonal channels (or a distorted crystalline structure). But, then what we have is not a stoichiometric tungsten oxide but rather a tungsten bronze with a very low residual ion or molecule content (or a reduced tungsten oxide).

Conclusion

We studied the formation of nanosized h-WO_3 during the annealing of HATB, $(NH_4)_{0.07}(NH_3)_{0.04}(H_2O)_{0.09}WO_{2.95}$ (sample **1**). We obtained new structural information concerning both the precursor HATB and the product h-WO_3. We detected three different positions of NH_4^+ ions and NH_3 molecules in HATB, which can be situated (i) at the surface of the particles, (ii) at a second kind of surface position or at the disordered spaces between crystallites, or (iii) at the hexagonal channels of the crystallites. The residual NH_4^+ ions and NH_3 molecules in the hexagonal channels seem to be vital for stabilizing h-WO_3: when they were completely released, the hexagonal framework collapsed in an exothermic reaction into m-WO_3. We propose that the structure of h-WO_3 cannot be maintained without traces of stabilizing ions or molecules in the hexagonal channels. This makes the existence of strictly stoichiometric h-WO_3 questionable.

Through adjusting the temperature and atmosphere of annealing of **1**, the composition (W oxidation state, residual NH_4^+ and NH_3 content) of h-WO_3 could be controlled. By this method, oxidized or reduced nanosized h-WO_3 samples can be prepared. The morphology of h-WO_3 can be controlled by selecting the appropriate HATB precursors. To study as to whether the composition of h-WO_3 influences its applications, the conductivity and gas sensitivity of as-prepared h-WO_3 samples with different compositions were measured. While indirectly it was observed by Raman and ^{1}H-MAS NMR that the composition had an influence on the

(52) Balázsi, C.; Pfeifer, J. *Solid State Ionics* **2002**, *151*, 353.
(53) Pfeifer, J.; Balázsi, C.; Kiss, B. A.; Pécz, B.; Tóth, A. L. *J. Mater. Sci. Lett.* **1999**, *18*, 1103.
(54) Daniel, M. F.; Desbat, B.; Lassegues, J. C.; Gerand, B.; Figlarz, M. *J. Solid State Chem.* **1987**, *67*, 235.

bulk resistance of different h-WO_3 samples, direct resistance measurements did not show this, probably because the resistance of powder samples was determined more by the surface of the particles than by the bulk. As-prepared h-WO_3 samples with different composition were tested as gas sensors of H_2S, and it was shown that the composition had a significant influence on the gas sensitivity of h-WO_3. In conclusion, we propose the use of ammonium tungstates in reactions that have been developed recently for producing h-WO_3 from alkaline tungstates. Through appropriate annealing of the products — in a similar way as in this study – h-WO_3 nanoparticles, nanowires, or nanotubes with a controlled composition can be prepared.

Acknowledgment. A diffractometer purchase grant from the Agency for Research Fund Management (KPI-EU-GVOP-3.2.1.-2004-04-0224/3.0 KMA) and a Hungarian GVOP-3.2.1.-2004-04-0210/3.0 grant are gratefully acknowledged.

CM800668X